

AD-R149 751

CARBON MONOXIDE ADSORPTION ON A PLATINUM ELECTRODE  
STUDIED BY POLARIZATION. (U) IBM RESEARCH LAB SAN JOSE  
CA K KUNIMATSU ET AL. NOV 84 TR-8 N00014-82-C-0583

1/1

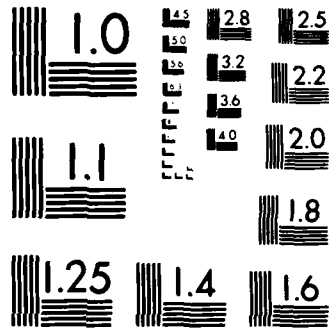
UNCLASSIFIED

F/G 7/4

NL

	END											

END



MICROCOPY RESOLUTION TEST CHART  
NATIONAL BUREAU OF STANDARDS-1963-A

AD-A149 751

DTIC FILE COPY

REPORT DOCUMENTATION PAGE		READ INSTRUCTIONS BEFORE COMPLETING FORM
1. REPORT NUMBER Technical Report No. 8	2. GOVT ACCESSION NO.	3. RECIPIENT'S CATALOG NUMBER
4. TITLE (and Subtitle) Carbon Monoxide Adsorption on a Platinum Electrode Studied by Polarization Modulated FT-IRRAS: I. CO Adsorbed in the Double Layer Potential Region and Its Oxidation in Acids		5. TYPE OF REPORT & PERIOD COVERED Technical
		6. PERFORMING ORG. REPORT NUMBER 12
7. AUTHOR(s) K. Kunitatsu, W. G. Golden, H. Seki and M. R. Philpott		8. CONTRACT OR GRANT NUMBER(s) N00014-82-C0583
9. PERFORMING ORGANIZATION NAME AND ADDRESS IBM Research Laboratory, K33/281 5600 Cottle Road San Jose, CA 95193		10. PROGRAM ELEMENT, PROJECT, TASK AREA & WORK UNIT NUMBERS
11. CONTROLLING OFFICE NAME AND ADDRESS Office of Naval Research 800 North Quincy Street Arlington, VA 22217		12. REPORT DATE November 1984
		13. NUMBER OF PAGES 16 + 8 figures
14. MONITORING AGENCY NAME & ADDRESS (if different from Controlling Office)		15. SECURITY CLASS. (of this report) Unclassified
		15a. DECLASSIFICATION/DOWNGRADING SCHEDULE
16. DISTRIBUTION STATEMENT (of this Report) Approved for public release; distribution unlimited.		
17. DISTRIBUTION STATEMENT (of abstract entered in Block 20, if different from Report) Approved for public release; distribution unlimited.		
18. SUPPLEMENTARY NOTES Prepared for publication in <u>Langmuir</u> .		
19. KEY WORDS (Continue on reverse side if necessary and identify by block number) Infrared Spectroscopy Electrode, Silver Electrolytes		
20. ABSTRACT (Continue on reverse side if necessary and identify by block number) Carbon monoxide adsorbed on a smooth platinum electrode was investigated in the potential range including the double layer region and the region of its steady state oxidation in solutions of 1M HClO <sub>4</sub> , H <sub>2</sub> SO <sub>4</sub> or HCl using <u>in situ</u> polarization modulated Fourier transform - IR reflection absorption spectroscopy (FT-IRRAS). The intensity, position and linewidth of the IR absorption band of the linearly adsorbed CO species were measured as a function of potential. The evolution of carbon dioxide produced by the oxidation of the adsorbed CO was observed <u>in situ</u> by monitoring the IR absorption spectrum of the carbon dioxide. Oxidation of the		

DTIC  
ELECTE  
JAN 31 1985

A

adsorbed CO is completed before the formation of a surface oxide or an adsorbed oxygen layer. It was found that the linear increase of the CO stretching frequency continued even into the CO oxidation potential region where the coverage of CO decreases appreciably. It is concluded that oxidation proceeds mostly at the edges of CO islands where the water molecules are adsorbed adjacent to the CO sites. The band due to CO adsorbed in the bridged form was observed in 1M HClO<sub>4</sub> by electrochemically modulated IR reflection spectroscopy (EMIRS) and it was concluded from its potential dependence that the bridged CO oscillator strength decreased at more positive potentials.

**CARBON MONOXIDE ADSORPTION ON A PLATINUM ELECTRODE  
STUDIED BY POLARIZATION MODULATED FT-IRRAS:  
I. CO ADSORBED IN THE DOUBLE LAYER POTENTIAL  
REGION AND ITS OXIDATION IN ACIDS**

K. Kunitatsu\*  
W. G. Golden\*\*  
H. Seki  
M. R. Philpott

IBM Research Laboratory  
San Jose, California 95193

**ABSTRACT:** Carbon monoxide adsorbed on a smooth platinum electrode was investigated in the potential range including the double layer region and the region of its steady state oxidation in solutions of 1M  $\text{HClO}_4$ ,  $\text{H}_2\text{SO}_4$  or  $\text{HCl}$  using *in situ* polarization modulated Fourier transform - IR reflection absorption spectroscopy (FT-IRRAS). The intensity, position and linewidth of the IR absorption band of the linearly adsorbed CO species were measured as a function of potential. The evolution of carbon dioxide produced by the oxidation of the adsorbed CO was observed *in situ* by monitoring the IR absorption spectrum of the carbon dioxide. Oxidation of the adsorbed CO is completed before the formation of a surface oxide or an adsorbed oxygen layer. It was found that the linear increase of the CO stretching frequency continued even into the CO oxidation potential region where the coverage of CO decreases appreciably. It is concluded that oxidation proceeds mostly at the edges of CO islands where the water molecules are adsorbed adjacent to the CO sites. The band due to CO adsorbed in the bridged form was observed in 1M  $\text{HClO}_4$  by electrochemically modulated IR reflection spectroscopy (EMIRS) and it was concluded from its potential dependence that the bridged CO oscillator strength decreased at more positive potentials.

\*IBM visiting scientist, 1983-1984. Permanent address: Research Institute for Catalysis, Hokkaido University, Sapporo, 060 Japan

\*\*IBM Instruments Inc., 40 West Brokaw Road, San Jose California 95110



Accession For	
NTIS GRA&I	<input checked="" type="checkbox"/>
DTIC TAB	<input type="checkbox"/>
Unannounced	<input type="checkbox"/>
Justification	
By	
Distribution	
Availability	
Restrictions	
1A1	

## INTRODUCTION

The nature of carbon monoxide adsorption on platinum electrodes and the mechanism of its oxidation have been studied extensively in the past mainly by electrochemical methods.<sup>1,2</sup> The idea of linear and bridge bonded adsorbed carbon monoxide species, CO(a), introduced by Gilman<sup>3</sup> for interpreting the electrochemical data, was based on the IR spectroscopic studies of the gas/metal interface by Eischens and Pliskin.<sup>4</sup> It is now generally agreed that when carbon monoxide adsorbs onto a platinum electrode under steady state conditions at potentials in the double layer region, the predominant species produced is linearly bonded CO(a) and the amount of the bridge bonded CO(a) is relatively small.<sup>1,3,5,6</sup>

On the other hand, it has been claimed by Breiter,<sup>7,8</sup> Brambow and Bruckenstein<sup>9</sup> and Cerwinski and Sobkowski<sup>2</sup> that, in addition to the dominant CO(a) species, a different chemical species, the nature of which is not known, is formed when carbon monoxide is allowed to interact with the platinized platinum surface at potentials in the hydrogen region. Species like carbon monoxide monohydrate (Stonehart<sup>10</sup>), or HCO type species (Kazarinov et al<sup>11</sup>), were also proposed for the adsorption of carbon monoxide in the hydrogen region.

The electro-oxidation of carbon monoxide adsorbed on platinum is known to be a complex process, the mechanism of which depends strongly on experimental conditions such as the potential of adsorption and the potential at which the oxidation is conducted. Therefore, one should be careful in comparing the mechanisms proposed by different authors.<sup>8,12-15</sup> The reactant-pair mechanism proposed by Gilman,<sup>12</sup> which involves a water molecule adjacent to a linearly adsorbed CO, corresponds to a case in which oxidation of the CO is complete before oxidation of the platinum electrode takes place.

On the other hand, McCallum and Pletcher<sup>15</sup> oxidized CO(a) by stepping the potential into the region where oxidation of the platinum surface took place simultaneously with CO(a) oxidation and they concluded that the oxidation of CO(a) took place at the perimeter of growing islands of platinum oxide.

The complexities of CO adsorption and its oxidation mechanism can now be studied much more directly by in-situ infrared reflection spectroscopy, which was first developed by Bewick et al.<sup>16,17</sup> Beden et al.<sup>17</sup> have studied the adsorption of CO on smooth platinum electrodes using EMIRS (Electrochemically modulated IR reflection spectroscopy) and later Russell et al.<sup>18</sup> utilized polarization modulated infrared reflection-absorption spectroscopy (IRRAS)<sup>19</sup> in a similar study. The CO stretching mode of the linearly adsorbed CO in the double layer region was observed and its frequency shift with electrode potential was confirmed.

Recently, we demonstrated that the combination of polarization modulated IRRAS and Fourier transform IR reflection absorption spectroscopy (FT-IRRAS)<sup>20</sup> can be used to detect a fraction of a monolayer of carbon monoxide adsorbed on a platinum electrode at potentials in the CO oxidation potential region.<sup>21</sup> In that investigation, CO was allowed to adsorb on the platinum electrode at a potential in the double layer potential region, *i.e.*, 0.4V(NHE).

The purpose of the present study is twofold: first, to investigate the nature of CO adsorbed on a Pt electrode in the double layer potential region and its mechanism of electrooxidation in various acid media *via in situ* polarization modulated FT-IRRAS; and, second to study the dependence of the linear CO(a) stretching frequency on electrode

potential in various aqueous media. The latter objective is stimulated by increasing theoretical interest in this phenomenon.<sup>22,23</sup>

We have found recently that both the electrochemical and spectroscopic nature of the CO(a) species produced when CO is allowed to interact with platinum at potentials in the hydrogen region are quite different from those adsorbed in the double layer region. However, these results will be reported in a separate paper.<sup>24</sup>

## EXPERIMENTAL

The results reported in this paper are based on measurements using two types of *in situ* IRRAS techniques; polarization modulated FT-IRRAS<sup>20</sup> and EMIRS.<sup>17</sup>

The polarization modulated FT-IRRAS experiments were carried out on an IBM Instruments Inc. IR/98 Fourier transform IR (FTIR) spectrometer. Design details and use of the electrolyte/electrode system is described elsewhere.<sup>25</sup> For most of the measurements reported here a spectro-electrochemical cell made from pyrex glass, similar in design to those of previous EMIRS studies<sup>16,26,27</sup> was used with a CaF<sub>2</sub> prism window. The window and the glass flange on which it was mounted were polished sufficiently flat so that no leakage of solution occurred. The platinum electrode was made by sealing a 99.95% pure Pt disk (20mmx1mm) into a soda glass piston, leaving one side of the disk exposed as the electrode surface. The surface of the electrode was polished successively with 1.0, 0.3 and 0.05 micron alumina on a polishing cloth.

The experimental arrangement used in the sample chamber of the FTIR spectrometer is illustrated in Figure 1. All FT-IRRAS spectra were taken with 4 cm<sup>-1</sup> resolution using either a HgCd/CdTe (Infrared Associates) or an InSb (Santa Barbara

Research Center) liquid  $N_2$  cooled detector. 300 scans (ca. 10 minutes) were taken for each spectrum in order to improve signal to noise ratio. A ZnSe photoelastic modulator (Hinds International) was used to modulate the polarization at 78 kHz.

The experimental details of the EMIRS technique have been described elsewhere.<sup>16,26</sup> A Si plate was used as the IR window for the cell. The angle of incidence of the IR beam at the electrode/solution interface was about  $45^\circ$ . The frequency of the potential modulation was 11 Hz.

The solutions were made up from organic-free water and either double distilled sulfuric acid, reagent grade hydrochloric acid or reagent grade perchloric acid. The reference electrode was Ag/AgCl (3M KCl saturated by AgCl) but all potentials reported here are in terms of the NHE scale. All experiments were carried out at room temperature.

After the solution had been deaerated by  $N_2$ , the Pt electrode was subjected to anodic-cathodic potential sweeps to clean the surface. Carbon monoxide was then bubbled through the solution to saturate the Pt surface by adsorbed CO molecules; the potential of the electrode being set to 0.4V. After approximately ten minutes, the potential of the Pt electrode was cycled between 0 and 1.5V several times to monitor the oxidation of the adsorbed CO. The Pt electrode was subjected to a final adsorption of CO at 0.4V before IR measurements were taken.

## RESULTS

1. Potential dependence of the FT-IRRAS spectra of linearly adsorbed CO on the Pt electrode in 1N  $H_2SO_4$ ,  $HClO_4$  and HCl. The FT-IRRAS spectra of CO adsorbed on a smooth platinum electrode in 1M  $HClO_4$  between 2000 and  $2150\text{ cm}^{-1}$  are shown as a

function of electrode potential in Figure 2. Since, at 0.8V the Pt electrode is free of adsorbed CO due to its oxidation to CO<sub>2</sub> a reference spectrum taken at 0.8V has been used for background subtraction to produce the spectra shown. The bands in this figure are assigned to the C-O stretching mode of linearly bonded CO species. The center of this band shifts to higher wave number at more positive potentials, while the intensity of the band remains constant and then decreases sharply after ca. 0.675V, due to the onset of electro-oxidation of the adsorbed carbon monoxide. This intensity decrease is due, presumably, to a decrease in CO coverage.

It is also possible to monitor the amount of carbon dioxide produced during the oxidation reaction at each potential. The change in the FT-IRRAS spectra of CO<sub>2</sub> is shown in Figure 3. These spectra are referenced to a spectrum of the electrode taken at 0.0V, a potential at which no CO<sub>2</sub> is produced. The detection of CO<sub>2</sub> owes to our use of the thin layer cell; the CO<sub>2</sub> is confined between the electrode and the window of the cell and detected by virtue of extension of the surface selection rule for some distance into the solution above the electrode.<sup>24</sup>

The band center position and integrated intensity of CO(a) and the integrated intensity of evolved CO<sub>2</sub> are plotted as a function of electrode potential in Figure 4a. There are four interesting features. First, the intensity of CO(a) remains constant until the onset of oxidation, indicating that the coverage of CO on Pt is constant until the CO is removed from the Pt surface by oxidation. Second, the band center position changes linearly with potential with a slope of about 30 cm<sup>-1</sup>/V, not only in the low potential region where the coverage of CO is constant but also through the potential region in which the CO coverage is decreasing. Signal to noise levels, however, do not allow the exclusion of a slight deviation from this linearity at very low coverage.<sup>21</sup> Third, the

evolution of carbon dioxide starts simultaneously with a decrease of the band intensity of CO(a) species, and last, the oxidation of CO(a) is completed by 0.7V, at which potential the oxidation of the electrode has not yet started.

These features, observed in perchloric acid, are also common to other acids such as sulfuric and hydrochloric acids. The data for these systems are shown in Figures 4b and 4c. The C-O stretching frequency and its shift with electrode potential coincide within 1 or 2  $\text{cm}^{-1}$  in the three acids as shown in Figure 5. The full width at half maximum is also plotted in this figure. It is clear that the band widths coincide to within ca. 1  $\text{cm}^{-1}$  in the three acids, becoming slightly smaller in the double layer region but then broadening when CO(a) is oxidized.

Although the nature of CO(a) on the platinum electrode formed at the double layer potential is quite similar in the three acids, there are also differences which can be seen in Figures 4a, 4b and 4c, *i.e.*, the potential region where the oxidation of CO(a) takes place is slightly different (it is lowest in sulfuric acid and highest in hydrochloric acid) and the absorption intensity of the CO(a) layer on platinum is the highest in perchloric acid and almost the same in the other two acids.

Consequently, the electrochemical behavior in the three acids was compared carefully by taking cyclic voltammograms of the CO(a) oxidation at a slow sweep rate of 1 mV/sec and by calculating the oxidation charge for each acid. In these measurements, after the adsorption of CO, the solution was purged by nitrogen gas for 20 minutes in order to eliminate contributions from CO dissolved in the solution. The resultant cyclic voltammograms are shown in Figure 6, from which it can be seen that the oxidation of CO(a) is completed by 0.7V in sulfuric and perchloric acids, which is consistent with the

IR spectroscopic data, while in hydrochloric acid the oxidation extends into a higher potential region where oxidation of the platinum surface takes place simultaneously. This higher measured potential for the oxidation is due to the fact that the oxidation of CO(a) on Pt in hydrochloric acid is so slow that a sweep rate of 1 mV/sec is not slow enough to maintain quasi-steady state conditions.

CO(a) oxidation charges were obtained by integration of the cyclic voltammograms in each solution of Figure 6. In the case of the hydrochloric acid, the difference in the current with and without CO(a) (upper and lower curves respectively in Figure 6c) was used to calculate the CO(a) oxidation charge. The results are shown in Table 1; CO(a) oxidation charge is given for a unit surface area. The effective electrode area was determined by integration of the cyclic voltammograms of the hydrogen region for each acid. The charge is nearly the same in sulfuric and hydrochloric acid while it is slightly higher, by ca. 5%, in perchloric acid; consistent with the IR intensity data.

The difference in the IR intensity of CO(a) and corresponding oxidation charge in the three acids can be explained by differences in anion adsorption. Perchlorate anions are known to be the least strongly adsorbed on Pt among the three anions. This is consistent with the fact that the IR absorption intensity and oxidation charge are highest in the case of the perchloric acid. The slow oxidation rate of CO(a) and the high CO oxidation potential in hydrochloric acid can be explained by the blocking of free surface sites by chloride anions. As will be discussed later, the free sites are necessary for adsorption of water molecules which are involved in the oxidation process.

2. EMIRS study of bridged CO species on Pt in 1M HClO<sub>4</sub>. A very weak and broad band in the region between 1800 and 1900 cm<sup>-1</sup> was seen in the FT-IRRAS spectra at

lower potentials, due to the bridge bonded CO(a) species on the platinum electrode. This band was more clearly detected, however, by the EMIRS technique. The EMIRS spectra of the bridge bonded CO(a) species on a smooth platinum electrode in 1M HClO<sub>4</sub> are given in Figure 7 for different modulation amplitudes starting from 0.05V. It is seen that the spectra show a bipolar nature for the smaller modulation amplitudes but exhibit a single signed shape at higher modulation amplitudes. The bipolar nature of the EMIRS spectra can be explained, as in the case of linearly adsorbed CO, as a result of the increase of the C-O stretching frequency when the potential is modulated to higher values. For comparison, the EMIRS spectrum of the linearly adsorbed species taken simultaneously are shown in Figure 8. The single signed nature of the bridged CO(a) spectra observed at higher modulation amplitudes can be explained by the considerable decrease of the band intensity at the higher potentials. The decrease of the band intensity is not caused by the oxidation of the bridged CO(a) species at the higher potentials, because the EMIRS spectrum of bridged CO(a) practically disappears once the potential is modulated into the CO oxidation potential region, viz. Figure 7. The decrease in intensity is more likely caused by the potential dependence of the C-O oscillator strength under constant coverage of the bridge bonded CO(a). A similar decrease of the C-O oscillator strength with an increase of positive electrode potential was seen much more clearly for bridge bonded CO(a) on a smooth palladium electrode by Kunimatsu<sup>26</sup> using a linear potential IRRAS method. It is interesting that the C-O oscillator strength decreases with an increase of positive potential for the bridged CO species while there is no such decrease observed for the linearly adsorbed CO species on a Pt electrode.

The results in Figure 7 and Figure 8 may indicate why the EMIRS spectra of CO species produced by the chemisorption of methanol, as first observed by Beden et al.,<sup>27</sup>

exhibit a bipolar nature for the linearly bonded CO species while it showing a single signed spectrum for the bridge bonded CO species, *i.e.*: The band intensity of bridge bonded CO(a) is approximately fifty times smaller than the intensity of the linearly bonded CO(a), as seen from a comparison of Figure 7 and Figure 8. This is why bridge bonded CO(a) species are difficult to detect in the FT-IRRAS measurements. Although it is not yet certain if the ratio of the intensity of the EMIRS spectra of the two forms of adsorbed CO accurately reflects the coverage ratio, the IR spectroscopic data obtained here supports the results of the electrochemical studies of two forms of carbon monoxide on the platinum electrode<sup>1,3,5,6</sup> and recent studies of CO adsorption on the platinum single crystal electrodes.<sup>28,29</sup>

## DISCUSSION

1. Origin of the CO(a) stretching frequency shift with electrode potential. The shift of the C-O stretching frequency with potential was observed by EMIRS by Beden *et al* for adsorbed CO produced by chemisorption of methanol onto a smooth platinum electrode.<sup>27</sup> Later, it was shown by Kunimatsu<sup>30</sup> and Russell *et al.*<sup>18</sup> that the integrated band intensity of the linearly adsorbed CO remained constant while the band center frequency shifted. Therefore, it was concluded that the dynamic coupling of the oscillating CO dipoles was not responsible for the frequency shift observed since a change in the coupling would require a change in CO(a) coverage on the platinum surface. The origin of the shift was explained qualitatively as being due to reduced back donation of metal electrons into the antibonding  $2\pi^*$  orbital of the adsorbed CO molecules as a function of increasing positive electrode potential which results in an increased C-O principle force constant. Recently, Holloway and Norskov<sup>23</sup> presented model calculations of the potential dependent frequency shift of CO(a) based on the argument

that the energy level of the antibonding state is shifted by the electrode potential thus affecting its occupancy. Assuming the adsorption parameters for CO on Ni under ultra-high vacuum (UHV) conditions, they showed that the linear shift of the C-O stretching frequency of  $30 \text{ cm}^{-1}/\text{V}$  could be obtained with one adjustable parameter.

On the other hand, Lambert has reported<sup>31</sup> that the applied electric field across the metal/gas interface gives rise to a decreased C-O stretching frequency due to the first order Stark effect, again for CO adsorbed on Ni(110) in a UHV system. The estimated vibrational Stark tuning rate is  $1.1 \times 10^{-6} \text{ cm}^{-1}/(\text{V}/\text{cm})$ , which could give rise to a significant shift of the C-O stretching frequency of adsorbed CO on electrodes due to the local electric field in the double layer. In his latest paper,<sup>32</sup> the frequency shift for adsorbed CO on a platinum electrode was estimated to be  $30+11 \text{ cm}^{-1}/\text{V}$  based on the Stark tuning rate of CO on Ni of  $1.1 \times 10^{16} \text{ cm}^{-1}/(\text{V}/\text{cm})$ . This value agrees very well with the results obtained here although the degree of closeness may be fortuitous.

*Ab initio* calculations of the wave functions for a cluster model of CO chemisorbed at an on top site of Cu(100) have been carried out both in the presence of an applied electric field and in a field free situation.<sup>33</sup> These calculations have confirmed Lambert's assignment of the C-O stretch frequency shift in an electric field as a Stark effect. Direct calculations of the vibrational frequency as a function of the applied field were compared with the Stark tuning rates obtained by substituting the values of  $a_1$ ,  $a_2$ ,  $M_1$  and  $M_2$  computed in the absence of a field in Eq. 12 of Ref. 32. It was found that these coefficients varied very slightly with the applied field (of the order of  $5 \times 10^6 \text{ V}/\text{cm}$ ). This is consistent with the linear potential dependence of the frequency shift. Coupled with our observation that the CO frequency and frequency shifts for three different acids are essentially identical implies that at any given electrode potential the field seen by the

CO molecule is not very different for the various anions. It is very significant that analysis of the computational results also indicate that there is very little change in the amount of 'back donated' electrons into the  $2\pi^*$  orbital of CO(a) as a result of an applied field. We therefore conclude that the linear potential dependent frequency shift observed here is mainly due to the first order Stark effect and the degree of back donation plays a minor role if any.

**2. Mechanism of CO(a) oxidation.** In view of the experimental results obtained in UHV systems, *i.e.*, that the stretching frequency of CO(a) on Pt decreases with decreasing surface coverage,<sup>34</sup> it is notable that in the electrochemical experiment, the linear dependence of the stretching frequency on electrode potential is observed well into the CO oxidation potential region (*viz.* Figure 4) where the CO surface coverage must certainly be decreasing. This implies, as in the UHV situation cited above, that the dipole environment of the adsorbed CO molecules is not changing and thus no dipole-dipole coupling frequency shifts occur as a function of average coverage. However, for CO adsorbed on Pt(111) in UHV, it was shown by Shigeishi and King<sup>35</sup> that exposing a full adlayer of CO to gaseous oxygen did not cause the CO(a) bandcenter to shift as the average CO coverage decreased due to oxidation. It was concluded that the oxidation of the CO(a) layer proceeded at the perimeter of CO(a) islands on the surface, leaving the dipole environment of the bulk of the CO(a) molecules unchanged.

The absence of a detectable decrease in the C-O stretching frequency and a very small change in the band linewidth during electro-oxidation (*viz.* Figure 5) strongly suggests that, for the CO adsorbed at the double layer potential, the dipole environment for the CO(a) molecules remains essentially unchanged during oxidation *i.e.*, as in the UHV experiments, the oxidation of the CO(a) to CO<sub>2</sub> occurs mostly at the edge of the

CO(a) islands. Also under the steady state conditions employed in the present *in situ* IR spectroscopic studies, the oxidation of CO(a) is completed before the oxidation of the platinum electrode occurs. Therefore, surface oxide is not involved in the CO(a) oxidation process. Thus, the most reasonable species which are involved in the oxidation of CO(a) are water molecules adsorbed at the edges of CO(a) islands. Thus, the reactant-pair mechanism proposed by Gilman<sup>12</sup> is consistent with the IR spectroscopic data obtained here, although the concept of the CO(a) island oxidation was not explicitly addressed in the mechanism. The oxidation mechanism, based on the present IR data, can be written as follows:



where  $(\text{Pt}-\text{CO(a)})_n$  represents a CO island and  $n$  is the number of linearly bonded CO molecules in the island. It is possible, however, that the adsorbed water molecules undergo further change to produce surface species such as O(a) or OH(a) which then react with the CO(a) island edges.

#### ACKNOWLEDGEMENTS

We wish to thank P. Bagus and W. Müller for stimulating discussions. This work was supported in part by the Office of Naval Research.

Table 1. Oxidation charge of CO(a) on Pt in three acids.

Acids	1M HClO <sub>4</sub>	0.5M H <sub>2</sub> SO <sub>4</sub>	1M HCl
$\mu\text{C}/\text{cm}^2$	331	306	314

## REFERENCES

1. Breiter, M. W. *J. Electroanal. Chem.* 1979, 101, 329.
2. Czerwinski, A; Sobkowski, J. *J. Electroanal. Chem.* 1978, 91, 47.
3. Gilman, S. *J. Phys. Chem.* 1963, 67, 78.
4. Eischens, R. P.; Pliskin, W. *Advances in Catalysis* 1958, 10, 18.
5. Brummer, S.B.; Ford, J. I. *J. Phys. Chem.* 1965, 69, 1355.
6. Bilmes, S. A.; De Tacconi, N. R.; Arvia, A. J. *J. Electroanal. Chem.* 1984, 164, 129.
7. Breiter, M. W. *J. Phys. Chem.* 1969, 73, 3283.
8. Breiter, M. W. *J. Phys. Chem.* 1968, 72, 1305.
9. Grambow, L.; Bruckenstein, S. *Electrochim. Acta*, 1977, 22, 377.
10. Stonehart, P. *Electrochim. Acta* 1973, 18, 63.
11. Kazarinov, W. E.; Andreyev, W. N.; Tsyachnaya, G. J. *Electrokhimiya* 1972, 6, 927.
12. Gilman, S. *J. Phys. Chem.* 1964, 68, 70.
13. Warner, T. B.; Schuldiner, S. *J. Electrochem. Soc.* 1964, 111, 992.
14. Kohlmayr, G.; Stonehart, P. *Electrochim. Acta* 1973, 18, 211.
15. McCallum, C.; Pletcher, D. *J. Electroanal. Chem.* 1976, 70, 277.
16. Bewick, A.; Kunimatsu, K.; Pons, B. S.; Russell, J. W. *J. Electroanal.* 1984, 160, 47.
17. Beden, B.; Bewick, A.; Kunimatsu, K.; Lamy, C. *J. Electroanal. Chem.* 1982, 142, 345.
18. Russell, J. W.; Overend, J.; Scanlon, K.; Severson, M.; Bewick, A. *J. Phys. Chem.* 1982, 86, 3066.
19. Golden, W. G.; Dunn, D. S.; Overend, J. *J. Catal.* 1981, 71, 395.
20. Golden, W. G.; Saperstein, D. D. *J. Elec. Spectrosc. Rel. Phenom.* 1983, 30, 43.
21. Golden, W. G.; Kunimatsu, K.; Seki, J. *J. Phys. Chem.* 1984, 88, 1275.

22. Ray, N. K.; Anderson, A. B. *J. Phys. Chem.* 1982, 86, 4851.
23. Holloway, S.; Norskov, J. K. *J. Electroanal. Chem.* 1984, 161, 193.
24. Kunimatsu, K.; Seki, H.; Golden, W. G.; Gordon II, J. G.; Philpott, M. R. to be published
25. Seki, H.; Kunimatsu, K.; Golden, W. G. *Appl. Spectrosc.* to be published.
26. Kunimatsu, K. *J. Phys. Chem.* 1984, 88, 2195.
27. Beden, B.; Lamy, C.; Bewick, A.; Kunimatsu, K. *J. Electroanal. Chem.* 1981, 121, 343.
28. Beden, B.; Bilmes, S.; Lamy, C.; Leger, J. M. *J. Electroanal. Chem.* 1983, 149, 295.
29. Motoo, T.; Furuya, N. Proc. Fall Conf. of Japan Electrochem. Soc. 1982, p 16.
30. Kunimatsu, K. *J. Electroanal. Chem.* 1982, 140, 211.
31. a) Lambert, D. K. *J. Electron Spec. and Rel. Phenom.* 1983, 30, 59.  
b) Lambert, D. K. *Phys. Rev. Letts.*, 1983, 50, 2106.
32. Lambert, D. K. *Solid State Commun.* 1984, 51, 297.
33. Bagus, P. S.; Müller, W.; Seki, H. to be published.
34. a) Shigeishi, R. A.; King, D. A. *Surf. Sci.* 1976, 58, 379. b) Crossley, A.; King, D. A. *Surf. Sci.* 1977, 68, 528.
35. Shigeishi, R.; King, D. A. *Surf. Sci.* 1978, 75, L397.

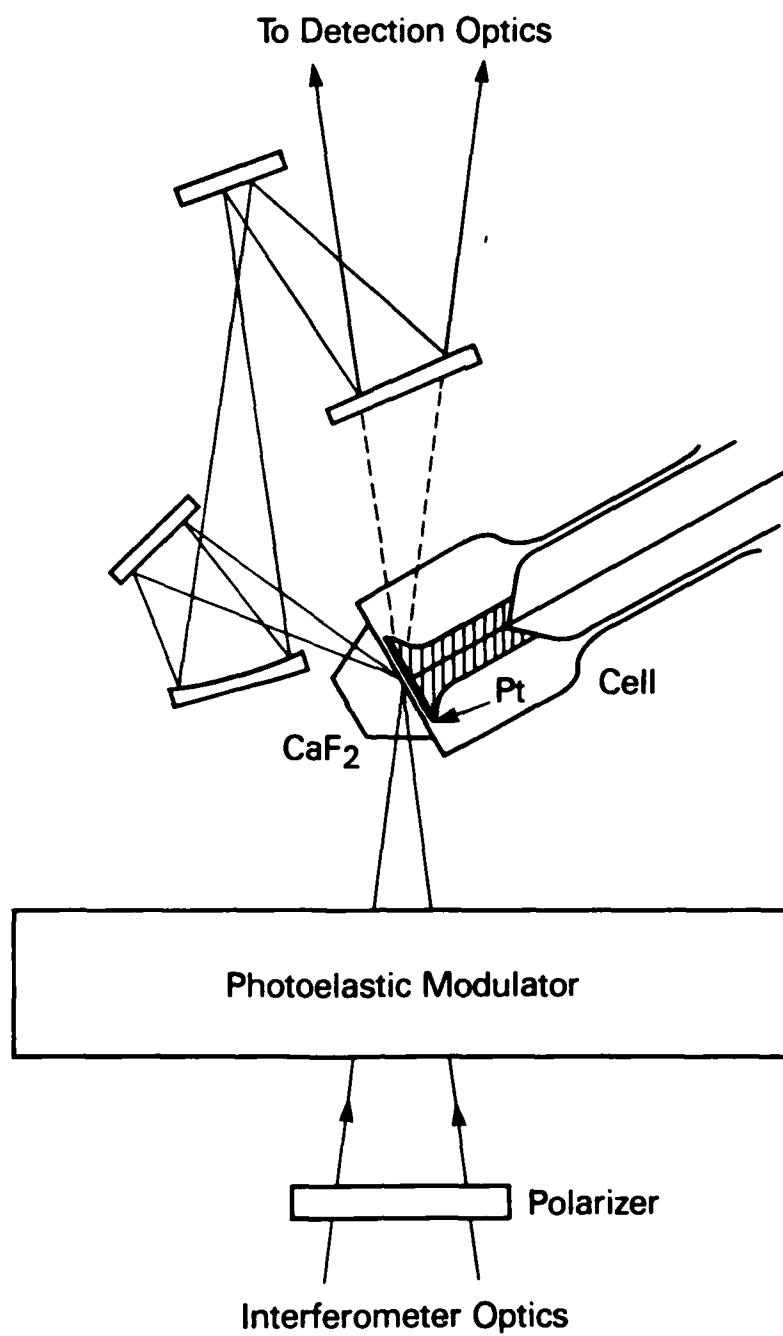


Figure 1. Optical arrangement of the polarization modulated IRRAS measurement in the FT-IR sample chamber.

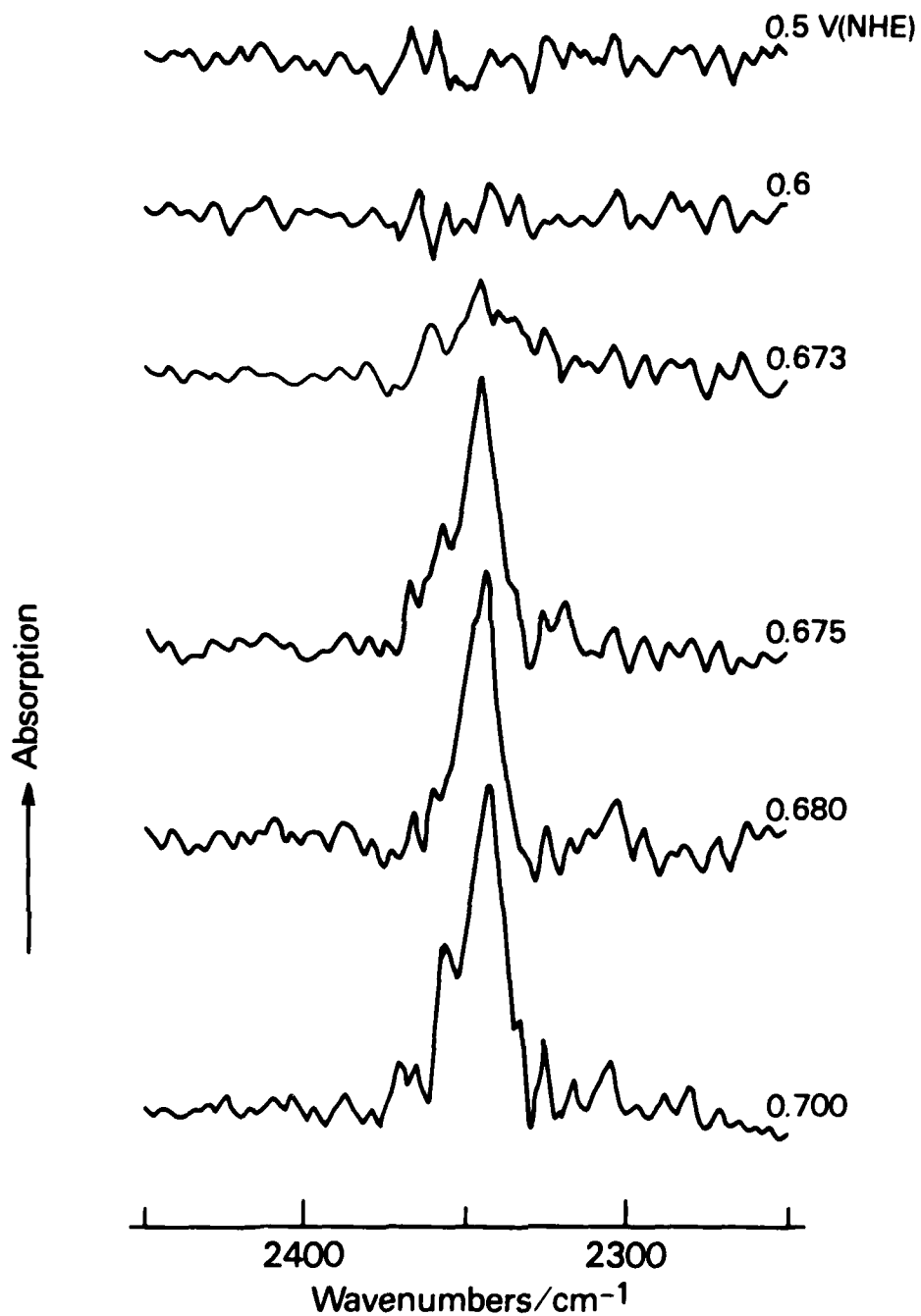


Figure 2. FT-IRRAS spectrum of linearly adsorbed CO on platinum in 1M HClO<sub>4</sub> as a function of electrode potential.

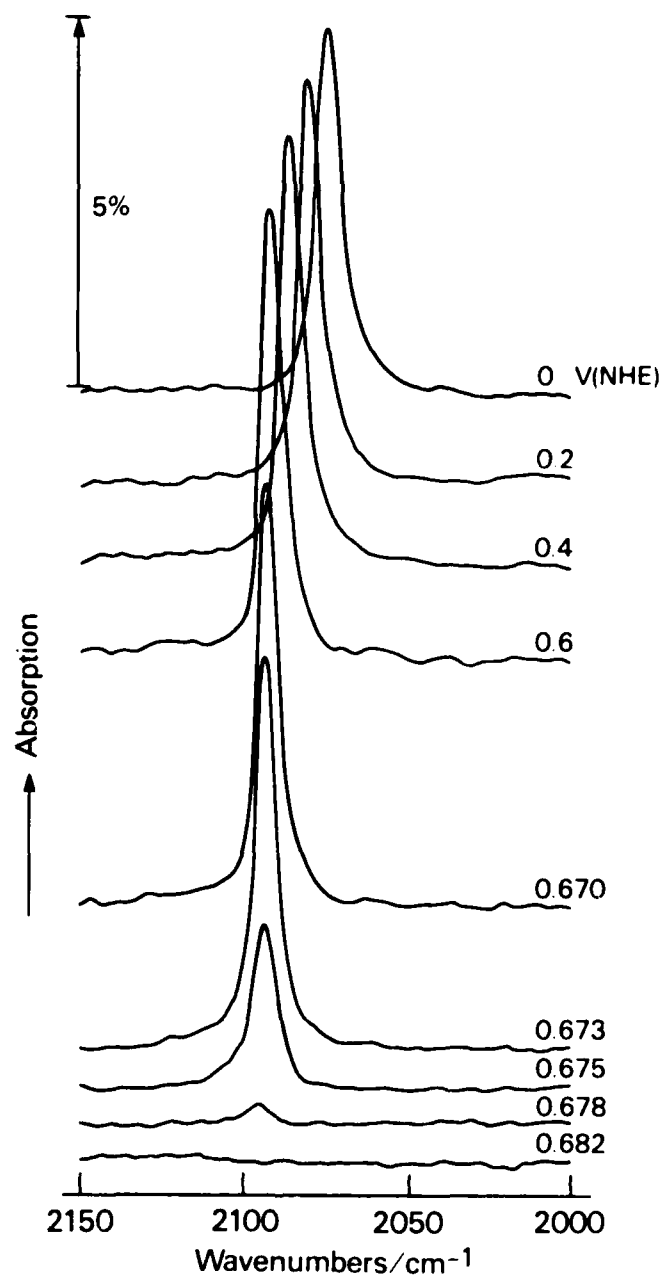


Figure 3. The FT-IRRAS spectrum of the carbon dioxide produced at each potential due to the oxidation of CO(a) in 1M HClO<sub>4</sub>.

(a)

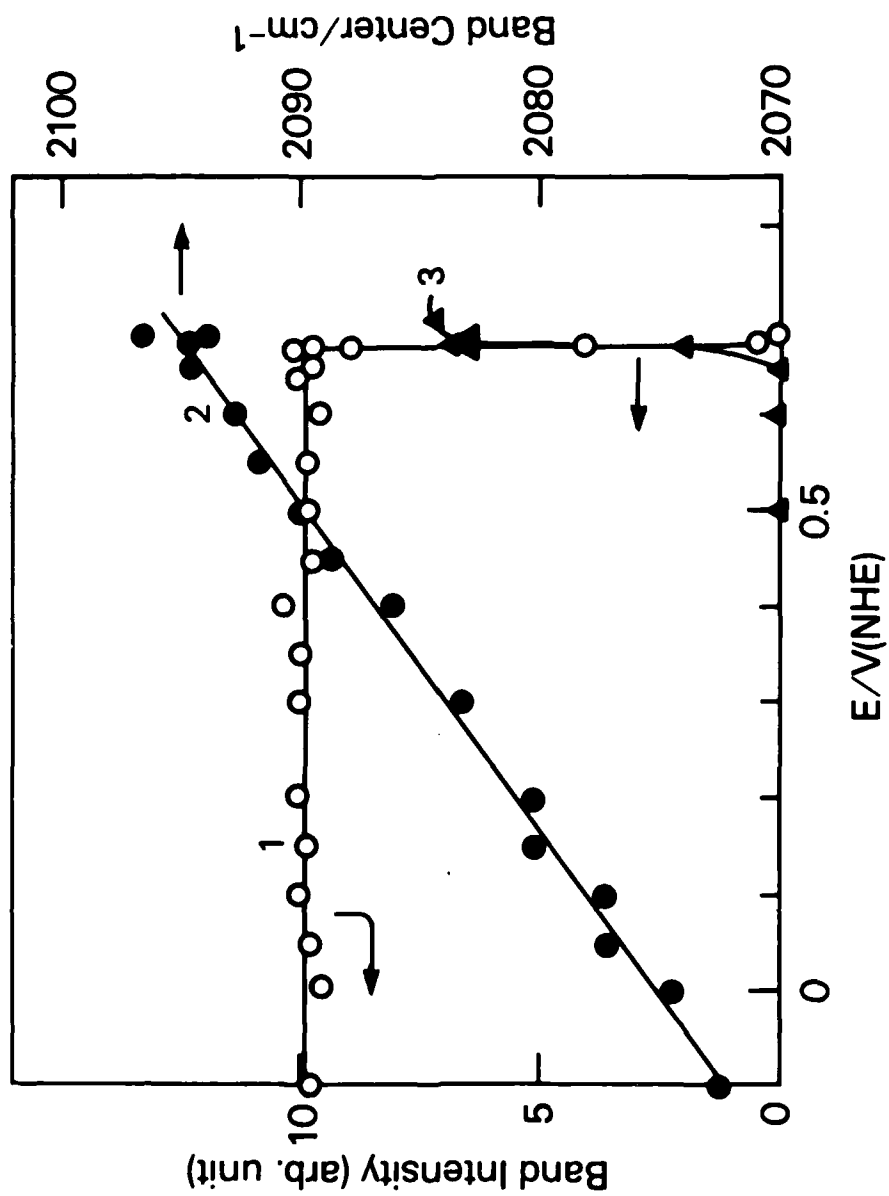


Figure 4. Plots of the integrated band intensity (1), the band center position (2) of the linearly adsorbed CO and the integrated intensity of the carbon dioxide (3) as a function of potential in (a) 1M HClO<sub>4</sub>, (b) 1M H<sub>2</sub>SO<sub>4</sub> and (c) 1M HCl.

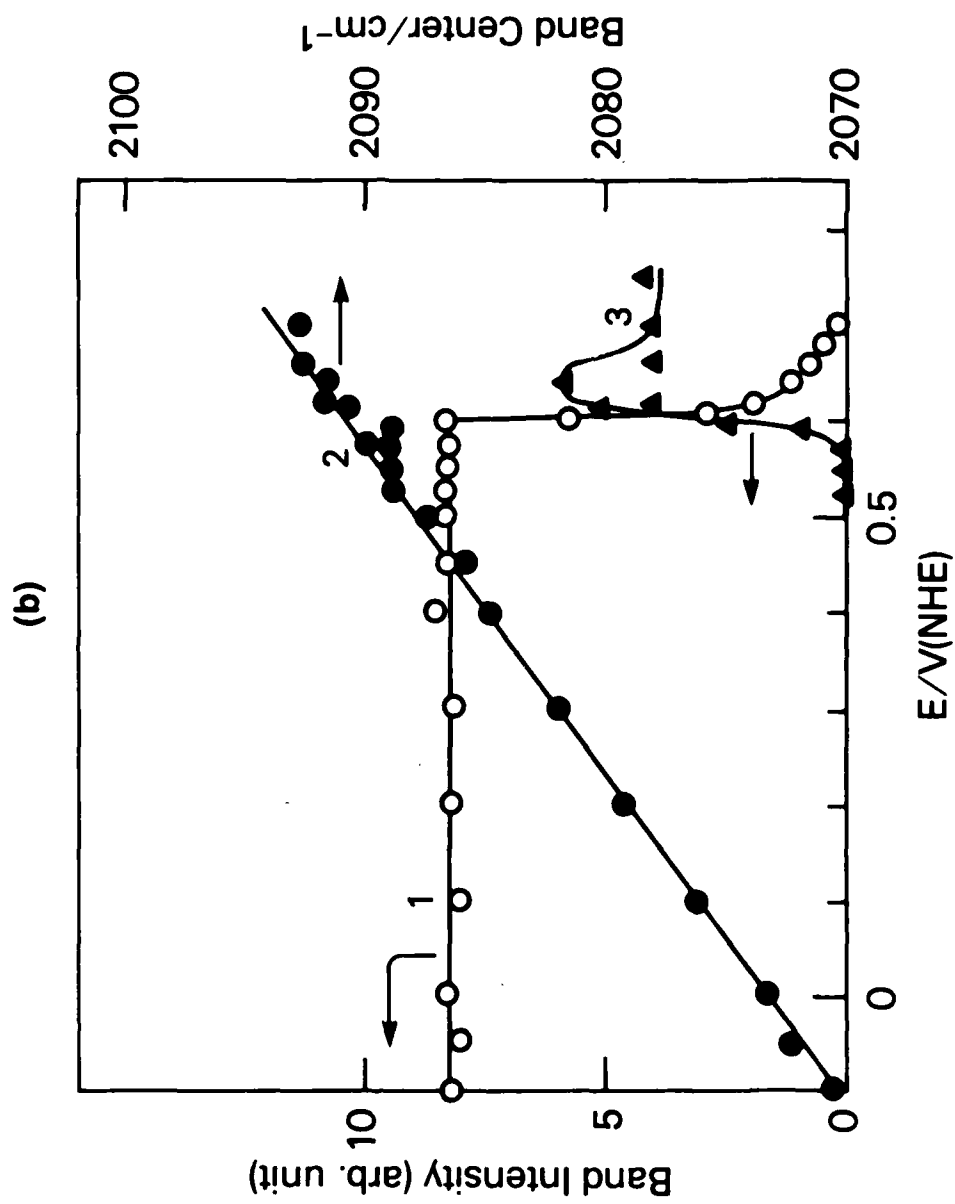


Figure 4. Plots of the integrated band intensity (1), the band center position (2) of the linearly adsorbed CO and the integrated intensity of the carbon dioxide (3) as a function of potential in (a) 1M HClO<sub>4</sub>, (b) 1M H<sub>2</sub>SO<sub>4</sub> and (c) 1M HCl.

(c)

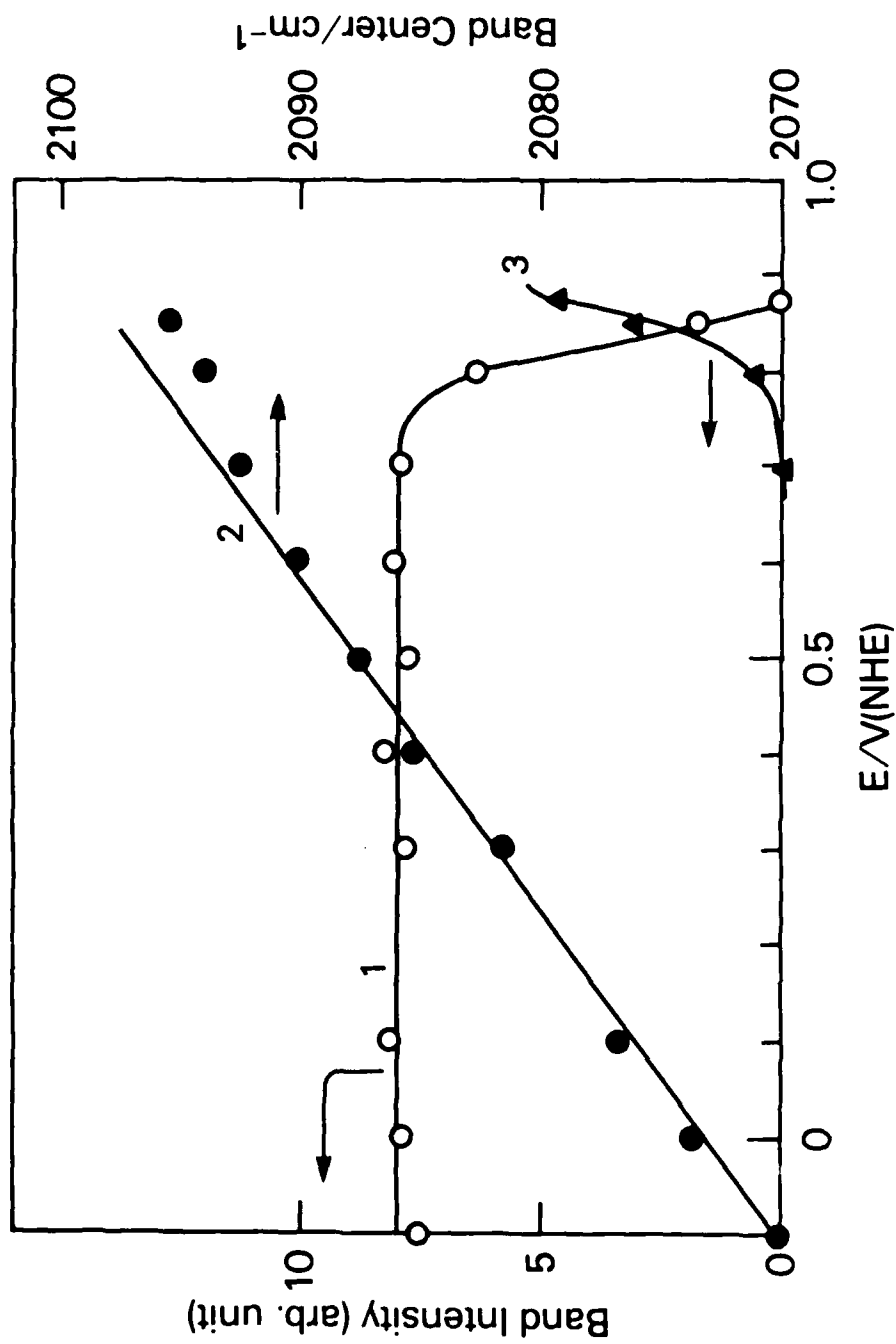


Figure 4. Plots of the integrated band intensity (1), the band center position (2) of the linearly adsorbed CO and the integrated intensity of the carbon dioxide (3) as a function of potential in (a) 1M HClO<sub>4</sub>, (b) 1M H<sub>2</sub>SO<sub>4</sub> and (c) 1M HCl.

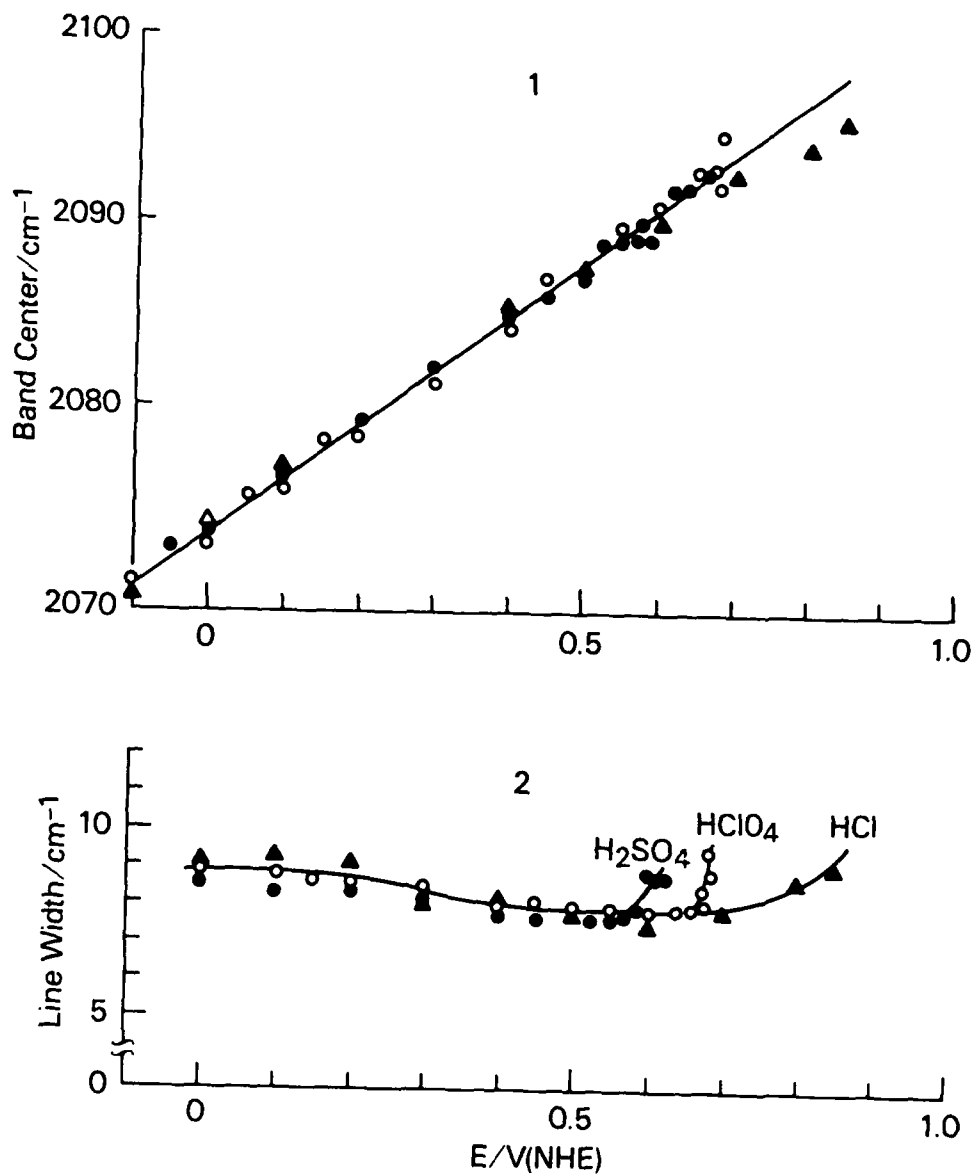


Figure 5. Plots of the band center (1) and of the band width (FWHM) (2) of linearly adsorbed CO on platinum versus potential in 1M HClO<sub>4</sub> (O), H<sub>2</sub>SO<sub>4</sub> (●) and HCl (X).

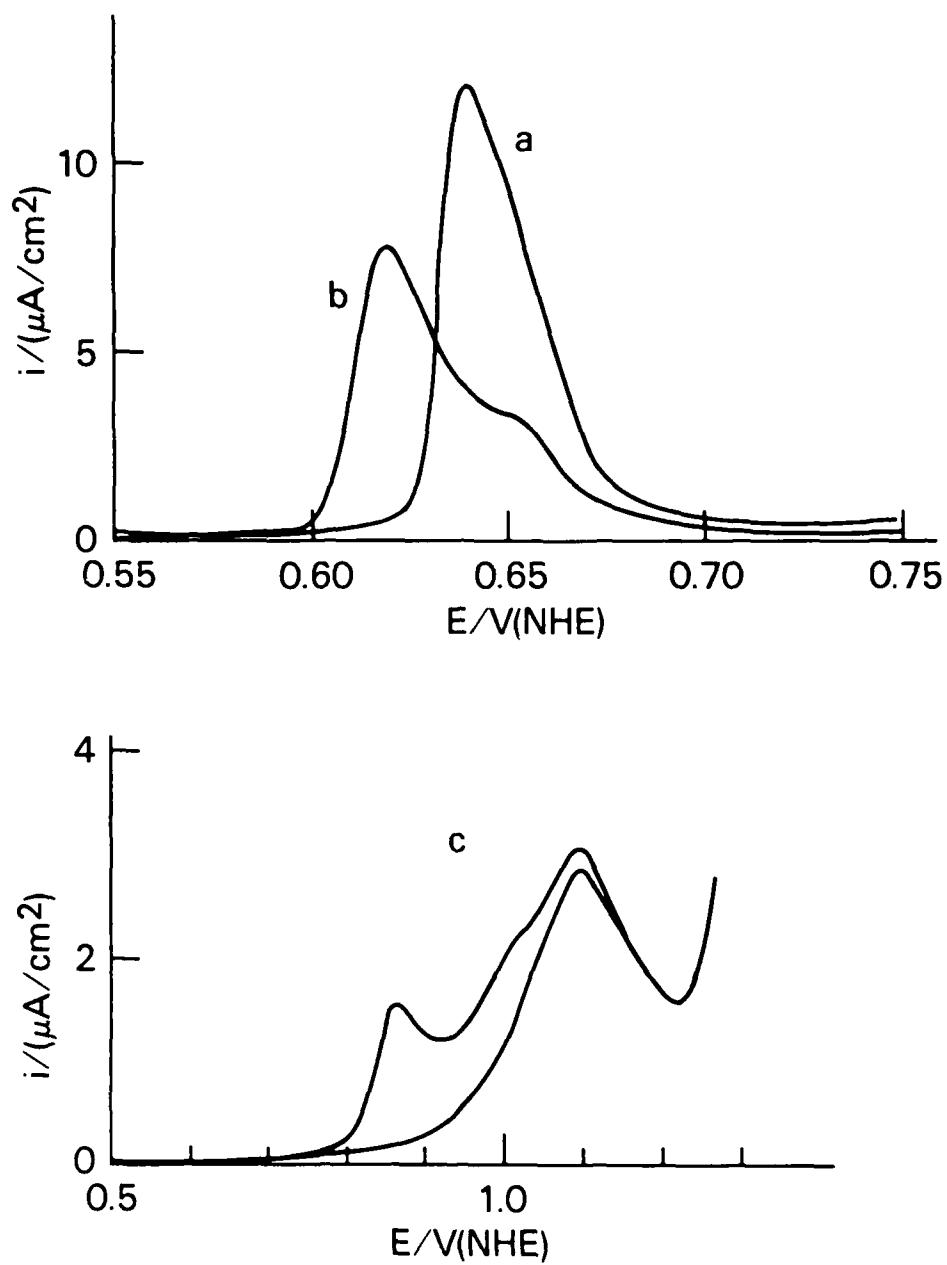


Figure 6. Cyclic voltammograms showing oxidation of CO(a) on platinum taken at 1 mV/sec. The solution was purged of CO by nitrogen gas after adsorption of CO. The lower curve in 1M HCl was taken immediately after the upper curve.

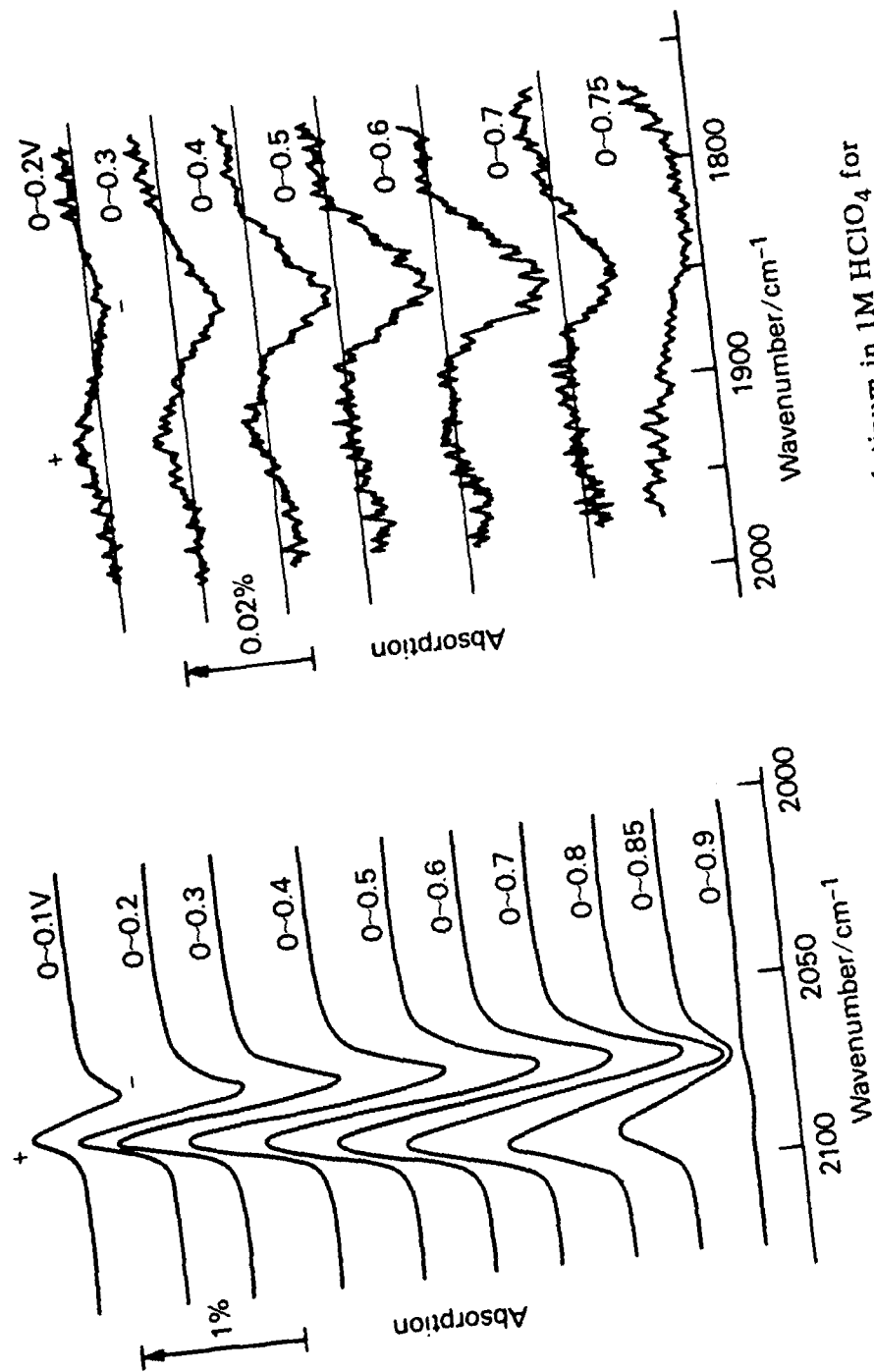


Figure 7. The EMIRS spectra of the bridged CO on platinum in 1M HClO<sub>4</sub> for various modulation amplitudes (11 Hz, 2-10 scans).

Figure 8. The EMIRS spectra of the linearly adsorbed CO on platinum in 1M HClO<sub>4</sub> for various modulation amplitudes (11 Hz, 2-10 scans).

**END**

**FILMED**

**3-85**

**DTIC**